Journal of Macromolecular Science, Part A
Publication details, including instructions for authors and subscription information:
http://www.informaworld.com/smpp/title~content=t713597274

Hybrid Nanocomposite Prepared by Graft Copolymerization of 4-Acryloyl morpholine onto Chitosan in the Presence of Organophilic Montmorillonite

Samia Al-Sigeny[a]; Manal F. Abou Taleb[b]; Nabil A. El-Kelesh[b]
[a] Chemistry and Physics Department, Faculty of Education at Kafr El-Sheikh, Kafr El-Sheikh University, Egypt [b] National Center for Radiation Research and Technology, Nasr City, Cairo, Egypt

To cite this Article Al-Sigeny, Samia , Abou Taleb, Manal F. and El-Kelesh, Nabil A.(2009) 'Hybrid Nanocomposite Prepared by Graft Copolymerization of 4-Acryloyl morpholine onto Chitosan in the Presence of Organophilic Montmorillonite', Journal of Macromolecular Science, Part A, 46: 1, 74 — 82
To link to this Article: DOI: 10.1080/10601320802515449
URL: http://dx.doi.org/10.1080/10601320802515449

Journal of Macromolecular Science®, Part A: Pure and Applied Chemistry (2009) **46**, 74–82

ISSN: 1060-1325 print / 1520-5738 online
DOI: 10.1080/10601320802515449

Taylor & Francis
Taylor & Francis Group

Hybrid Nanocomposite Prepared by Graft Copolymerization of 4-Acryloyl morpholine onto Chitosan in the Presence of Organophilic Montmorillonite

SAMIA AL-SIGENY,[1] MANAL F. ABOU TALEB[2,*] and NABIL A. EL-KELESH[2]

[1]*Chemistry and Physics Department, Faculty of Education at Kafr El-Sheikh, Kafr El-Sheikh University, Egypt*
[2]*National Center for Radiation Research and Technology, P.O. Box 29, Nasr City, Cairo, Egypt*

Received April 2008, Accepted July 2008

Organophilic montmorillonite (OMMT) was synthesized by cationic exchange between Na-MMT and Vinyl benzyl triphenyl phosphonium chloride in an aqueous solution. A new nanocomposite consisting of 4-acryloyl morpholine-chitosan and OMMT was prepared by γ-ray irradiation polymerization. The intercalation spacing of these nanocomposites was investigated with X-ray diffraction and its thermal stabilities by adding nanocomposites were characterized by thermal gravimetric analysis. The nanocomposites showed improved resistance to water absorption. The most interesting application of the nanocomposite is its ability for adsorption purification of waste water containing acid dyes. One of the objectives in this study was to develop new and active prepared copolymers which can be examined for their antimicrobial activities. It was found that the copolymer nanocomposite based on phosphonium group and some heavy metal ions in its structure having broad spectrum against pathogenic bacteria such as Staphylococcus aurius, Escherichia coli and Aspergillus flavus fungi.

Keywords: Nanocomposites, chitosan, 4-acryloyl morpholine, OMMT, γ-ray irradiation, adsorption, acid dyes, antimicrobial activity

1 Introduction

In recent years, polymer/clay nanocomposites have received considerable attention because they combine the structure, physical and chemical properties of both inorganic and organic materials. Compared to the pure polymers these nanocomposites demonstrate excellent properties such as improved storage modulus (1), decreased thermal expansion coefficients (2), reduced gas permeability (3), and enhanced ionic conductivity (4). Recently, the field of material science has witnessed the emergence of both hydrogels and a novel class of materials called organic–inorganic hybrids. Hydrogels and hybrid materials are of intensive interest in contemporary material chemistry as these materials have potential applications in biomedical devices, matrices for drug delivery systems, carrier for cells immobilization, carrier for signaling molecules, and bioseparation membranes (5–10). The hybrids having such combined characteristics of organic and inorganic substances promise new high performance or high functional materials to fully exploit this technical opportunity with benefits of the better of the two worlds.

*Address correspondence to: Manal F. Abou Taleb, National Center for Radiation Research and Technology, P.O. Box 29, Nasr City, Cairo, Egypt. E-mail: abutalib_m@yahoo.com

The clay that is most generally used is montmorillonites (MMT) belongs to the 2:1 layered silicate. Their crystal lattice consists of two silica tetrahedral sheets fusing into an octahedral sheet. Isomorphous substitutions of Si^{4+} for Al^{3+} in the tetrahedral lattice and of Al^{3+} for Mg^{2+} in the octahedral sheet can generate negative charges that are counterbalanced by cations such as Ca^{2+} and Na^{+}. Many cationic surfactants can easily exchange with the hydrated cations between the layers and render the clay more organophilic for the very weak force holding them. As the surface energy of the organoclay is much lower, many polymers and monomers can easily intercalate within the galleries.

Chitosan is one of the most abundant natural aminopolysaccharides. It has been widely used in food production for clarification and deacidification of fruit juices (fining agent), for purification of water, for antioxidative maintenance in muscle foods, etc., (11) and in pharmaceutical areas, e.g. for drug-delivery systems (12) because it has good biocompatibility, biodegradability, film-forming property and antimicrobial activity (13). In order to widen its application, many attempts have been made to optimize its properties, such as by cross-linking (14), blending (15–17) and formation into chitosan based composites (18).

Synthesis of polymer nanocomposites has typically involved either intercalation of a suitable monomer followed

by *in situ* polymerization(19,20) or intercalation polymerization from solution (21). According to this method, monomer molecules are first introduced into the galleries and then polymerized inside the layers.

A more recent approach was realized by surface modifications that kill microbes on contact without releasing an exhaustible antimicrobial compound. The polymeric antimicrobial nanocomposite is a special case where the surface-active group is bound to a polymer. The most studied and widely used polymeric antimicrobial nanocomposite are based on quaternary ammonium compounds (QACs), which are known as good antimicrobial agents. Two molecular groups are needed for their activity: a cationic group and a polar alkyl chain. These two groups are responsible for the bactericidal activity of QACs, which is based on disruption of bacterial cell membranes. This leads to leaking of important constituents of the cytoplasm, and problems with homeostasis; e.g. disturbed metabolism and disrupted replication.

Development of other cationic antimicrobials has been reported. These compounds are quaternary phosphonium compounds and quaternary sulfonium compounds (22, 23). The former compounds are reported to be more efficient than QACs. It is quite remarkable that quaternary phosphonium compounds are more effective against S. aureus than E. coli, because S. aureus is normally more resistant to antimicrobials than E. coli. This higher efficiency may be due to the cell wall composition. Polymeric quaternary sulfonium compounds exhibit high bactericidal activity, but they lack thermal stability and therefore commercial use is not likely. Quaternary phosphonium compounds exhibit higher bacterial activity than quaternary ammonium compounds, but are much more expensive and are therefore not widely used.

In present work, describe the synthesis of chitosan/4-acryloyl morpholine/organophilic montmorillonite nanocomposites initiated by γ-ray irradiation polymerization. Graft copolymerization and the intercalation of (ACMO) occurred at the same time. The objectives of this study are to investigate the effects of prepared nanocomposite on the structural, thermal, and the removal effects for two acid dyes using CS/ACMO/OMMT nanocomposites and additionally, to investigate the antimicrobial activity of the copolymer and its nanocomposits. In this work two important bacteria are discussed; Gram-positive, Gram-negative Bacteria and Fungi.

2 Experimental

2.1 Materials

Chitosan (CS) was kindly by pronova Biopolymer, Inc (USA). The degree of deacetylation and molecular weight were determined as 85% and 50,000, respectively. 4-acryloyl morpholine (ACMO) was purchased from Aldrich Chemical Co. (Milwaukee, U.S.). The clay mineral used in this study was sodium montmorillonite. Triphenyl phosphine was purchased from Aldrich Chemical Co.

2.2 Dyes

Each of the following dye solutions was prepared initially by dissolving 0.10 g in one liter from distilled water to prepared 100 mg/l. The concentration of the dye was measured and determined by UV spectroscopy (UNICAM UV/Vis Spectrometer. 1000 Model). The types of dyes used were Acid fast yellow G and Acid green B dye (Dyestuffs and Chemicals Co., Kaffer El-Dawar, Egypt) as seen below:

Dyes	*Structure formula*	*I.C.*
Acid fast yellow G	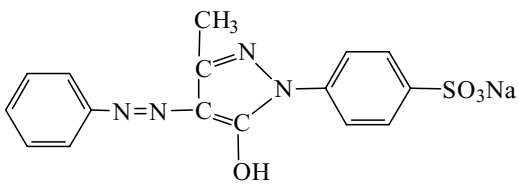	A/YEL/11
Acid Green B	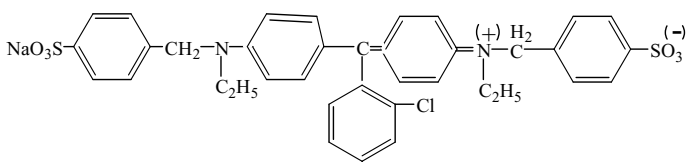	A/GR/16

2.3 Preparation of Phosphonium Cationic Monomer

A mixture of vinyl benzyl chloride (12.3 gm; 8.05 mol) was added to a solution of triphenyl phosphine (21.15 gm; 8.05 mol) in 15 ml dry diethyl ether, and heated overnight at 50°C under a nitrogen inlet. The solid product was washed several times with dry ether. Vinyl benzyl triphenylphosphonium chloride (VBTPCl) monomer was prepared from triphenyl phosphine and vinyl benzyl chloride in presence of diethyl ether as solvent (25) (Mulvancy and Chang, 1977) (Scheme 1).

2.4 Preparation of OMMT

OMMT was prepared by cationic exchange between Na^+-MMT galleries and VBTPCl. The suspension of 1 g of

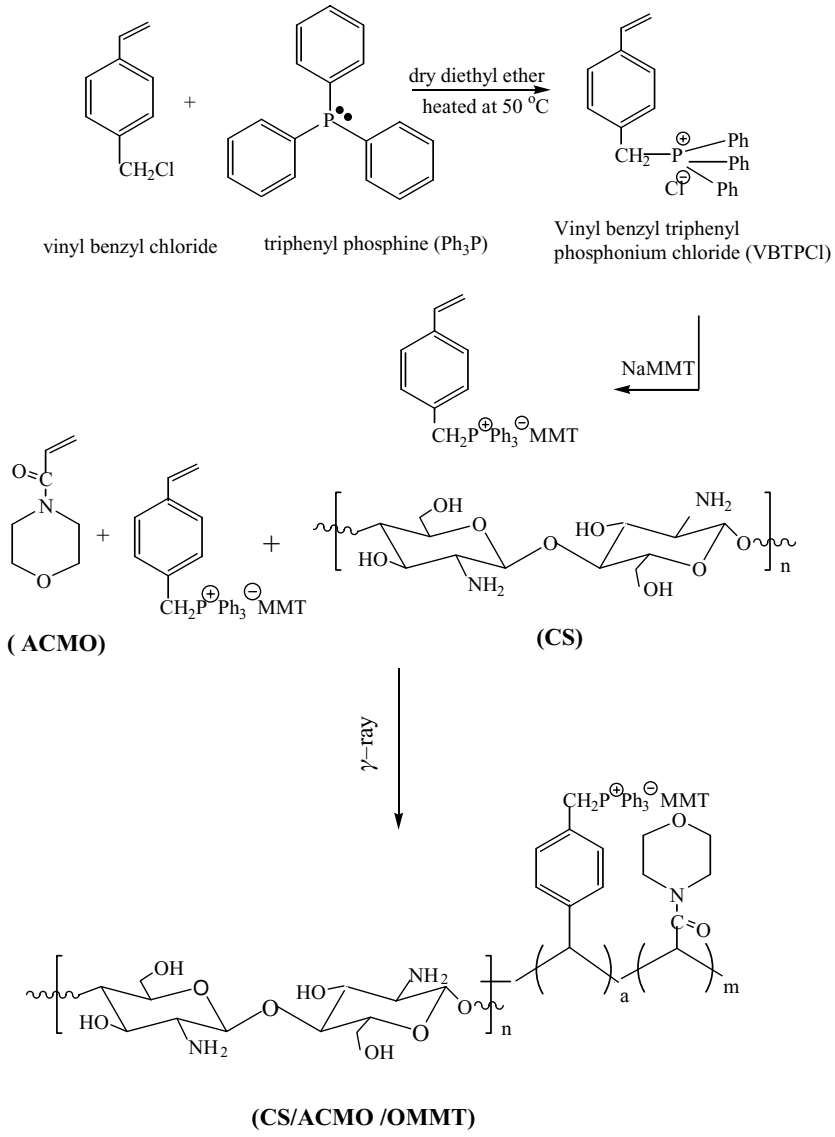

Sch. 1. Schematic illustration of the nanocomposite synthesis.

Na^+-MMT in 30 ml distilled water was stirred overnight. To the stirred suspension 4 g of Vinyl benzyl triphenyl phosphonium chloride (VBTPCl) monomer (VBTPCl) was soluble in (11 ml H_2O: 2.5 ml dioxane) was added dropwise and the stirring was continued for 24 h at room temperature. The exchanged OMMT was filtered and washed with distilled water until no chloride ion was detected with 0.1M $AgNO_3$ solution. Then the product was dried in vacuum oven at 70 °C for 12 h. The OMMT was obtained and then was ground with a mortar.

2.5 Synthesis of CS/ACMO/OMMT Nanocomposites

An exact amount of chitosan was first dissolved in 1% acetic acid to prepare 2 wt% solutions using a 50 cm^3 stoppered bottle, followed by the addition of 3.0 g monomer 4-acryloyl morpholine (ACMO). The nanoparticle loadings were varied as 0%, 1%, 3% and 5% of the combined weight of the monomer and chitosan. After constant stirring for 30 min, the system was deoxygenated by slow bubbling of nitrogen gas through the solution for 10 min. The sample bottles were irradiated for a specified time in a ^{60}Co γ-ray (dose: 10 kGy; dose rate: 2.86 Gy/s). After completion of the reaction, the contents were cooled and cast on a glass plate, the solvent was then evaporated and sample films were obtained. The conversion of ACMO was determined by the following equation:

$$\text{Conversion}\% = [\text{Sample disc(g)} - \text{OMMT(g)} - \text{Chitosan (g)/ACMO used(g)}] \times 100$$

2.6 Characterization of Nanocomposites

X-ray diffraction patterns were obtained with XD-DI Series, Shimadzu apparatus using nickel-filtered and Cu-Kα target. This technique was performed to clarify the changes in morphological structure caused by the copolymerization of different comonomer compositions.

Thermal Gravimetric Analysis (TGA) was conducted on a Shimadzu TGA system of Type TGA-50 in nitrogen atmosphere 20 ml/min was used in this study. The temperature range was from ambient to 30–600°C at heating rate of 10°C/min.

IR spectrum was recorded on a Mattson 1000, Unicam, England spectrometer scanning from 4000 to 400 cm^{-1} at room temperature. The samples were ground with KBr crystal and the mixture of them was pressed into a flake for IR measurement.

The ESR patterns were recorded at room temperature on an EMX-9.76 GHZ Bruker spectrometer (Germany). The recording parameters were used for OMMT and CS/ACMO/OMMT (reference sample): microware power 10.08 mW, microwave frequency 9.777 GHz, magnetic sweep width 200.000G, modulation Amplitude 6.00 G, time constant 163.84 ms.

The morphology of the nanocomposites was imaged using a SEM; JEOL-JSM-5400 scanning electron microscope–Japan. The specimen was coated with gold for improved scanning electron microscopy.

2.7 Water Uptake Measurements

The clean, dried sample films of known weights were immersed in distilled water at 25°C until equilibrium was reached (almost 24 h). The films were removed, blotted quickly with absorbent paper and then weighed. The uptake percentage of these samples was calculated using the equation:

$$\text{Swelling}\% = [(w_s - w_d)/w_d] \times 100$$

Where w_d and w_s represent the weights of dry and wet hydrogels, respectively.

2.8 Adsorption Study

About 0.1 g of the CS/ACMO/OMMT nanocomposites was immersed in the acid dyes solution of definite concentration (100 ppm) at room temperature until the complete absorption. The concentration of the dyes solution was measured by UV spectroscopy.

2.9 Antimicrobial Testing

Gram-positive cocci, as well as staphylococcus auries, microorganism was extracted, isolated and supplied from, bacteriology lab, microbiology department., NCCRT, Atomic energy authority, Cairo, Egypt. Nutrient agar (OXOID) was supplied from Hampshire, England. The prepared nanocomposites (0.1 g) were tested against gram positive; Staphylococcus aurius, gram negative bacteria; Escherichia coli and Aspergillus flavus fungi were used. The assay plates were seeded with the test organisms (3–5 $\times$ 10^5 c.f.u./ml) After agar solidification the wells were filled with 0.1 g of polymer discs. Plates were incubated at 30°C for 2 days in the case of bacteria and fungi. The antimicrobial activities were represented by the diameters of the inhibition zone (cm).

The total uncertainly for all experiments was in the range 3–4%.

3 Results and Discussion

The present work describes the synthesis of the OMMT which is more interested step in synthesis of polymer–MMT nanocomposites. Firstly, vinylbenzyl triphenyl phosphonium group is often used as they are very effective agents for modifying clays by ionic bond between them through the exchange of Na cation in MMT interlayer with phosphonium group. The presence of phosphorous atom P was confirmed by elemental analysis. Secondly, the OMMT opens the gallery spacing which allowed monomers and polymers to be enter more easily. A schematic illustration of the nanocomposite synthesis is shown in Scheme 1.

3.1 Influence of OMMT on Monomer Conversion

Figure 1 shows the relationship between irradiation dose and monomer conversion. It can be seen that below 5 kGy, conversion of ACMO dramatically increases with increasing dose. After the conversion of ACMO reaches about 80%, the viscosity increases in the system and lowering monomer concentration lead to decrease the

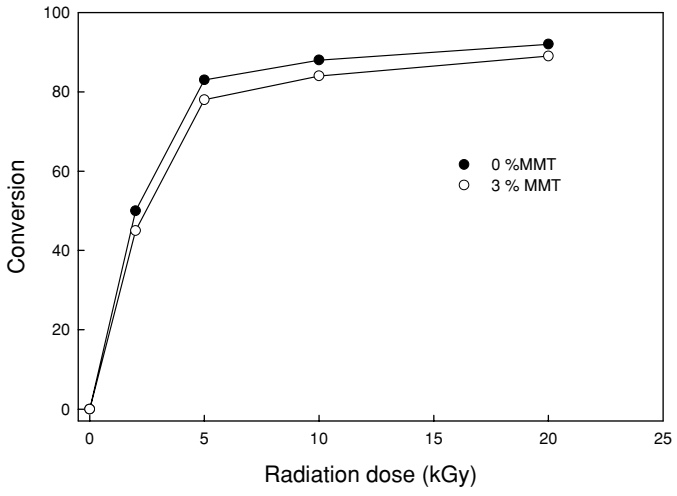

Fig. 1. The monomer conversion percent vs. radiation dose of CS/ACMOand CS/ACMO/OMMT; at dose rate: 2.86 Gy/s.

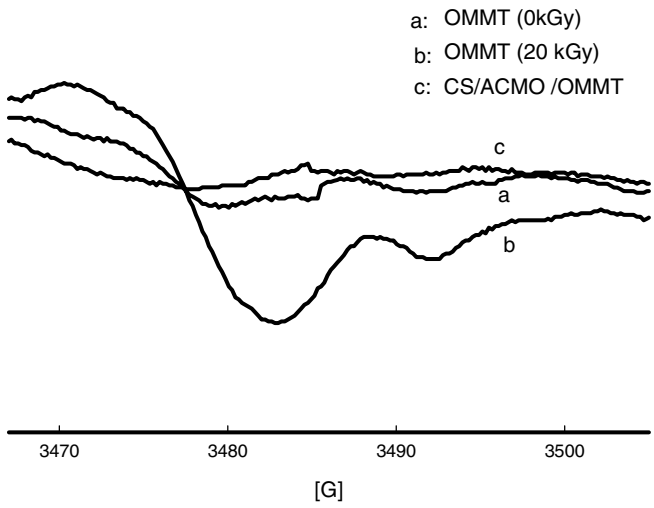

Fig. 2. ESR spectra of CS/ACMO/OMMT and OMMT before and after irradiation.

polymerization rate. This result was due to the restricted movement of ACMO and the inhibition of the propagating chain radicals in the OMMT galleries. Therefore, the polymerization rate of ACMO will be decreased which concerned with the conversion of ACMO in the OMMT system that was lower than in the pure system.

A large amount of free radicals of OMMT are produced when the OMMT is exposed to γ-ray irradiation (Fig. 2). These free radicals of the OMMT can combine with propagating chain radicals, and the movements of ACMO monomers and the propagating chain radicals are inhibited owing to the OMMT galleries. Then the polymerization rate of ACMO decreases. Therefore, the conversion of ACMO in OMMT system is lower than the pure ACMO.

3.2 FTIR for Characterization Structure

The FTIR spectrum of the polymer–clay (Fig. 3) shows the characteristic bands at 1433 cm^{-1} (the planar P–C_{phenyl} bonds), 1150 cm^{-1} (the stretching vibrations of the C_{phenyl}–H bonds) and 1070 cm^{-1} (P–O bonds) corresponding to the phosphonium salt attached to phenyl group. These observed bands are discussed by many authors before (21, 25). Comparing these bands characteristic for phoshonium salt of the copolymer and with the clay added, the results showed a shift from 1070 to 910 cm^{-1}. It's cleared that the feasibility to explain and confirme of phosphonium salt to be intercalated with metal oxide by appearing P–O band was possible (5, 21). The broadness of this characteristic band is apparently related to intermolecular interaction. The IR peaks at 915, 875 and 836 cm^{-1} are attributed to AlAlOH, AlFeOH and AlMgOH vibration (26, 27) in polymer-clay.

3.3 XRD of Nanocomposites

It was reported that XRD spectra of pure chitosan have two prominent crystalline peaks at (2θ) 10° and 20° (28). In chitosan crosslinked with ACMO more suppressed peaks

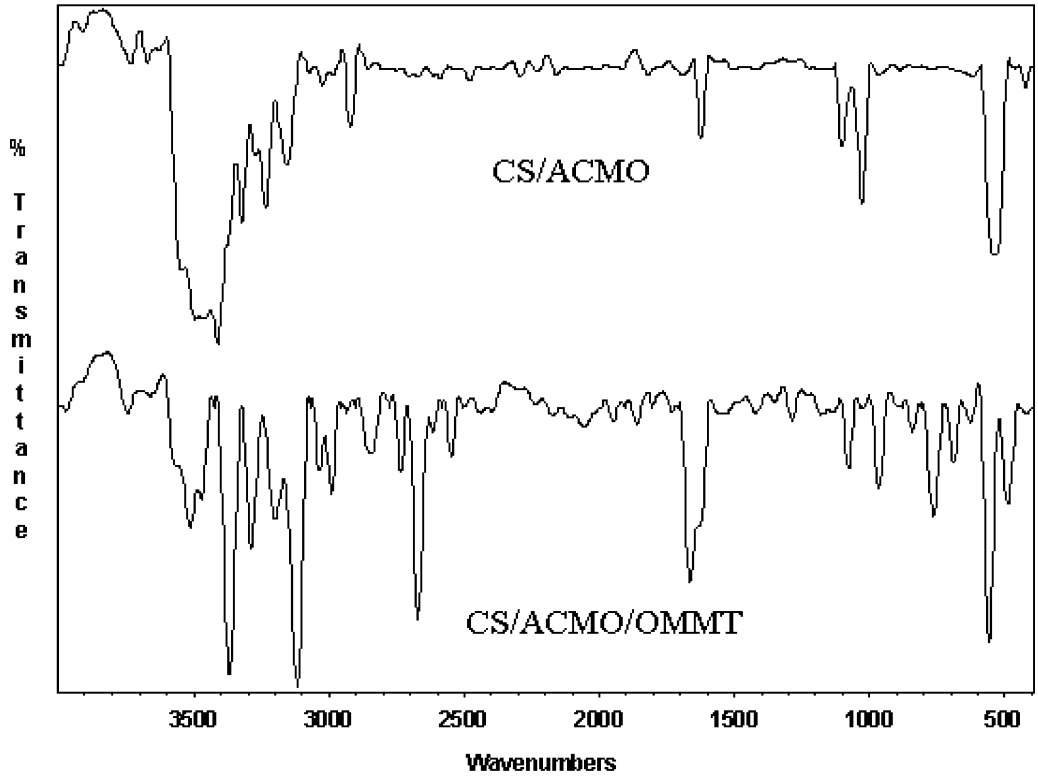

Fig. 3. IR spectra of CS/ACMO and CS/ACMO/OMMT.

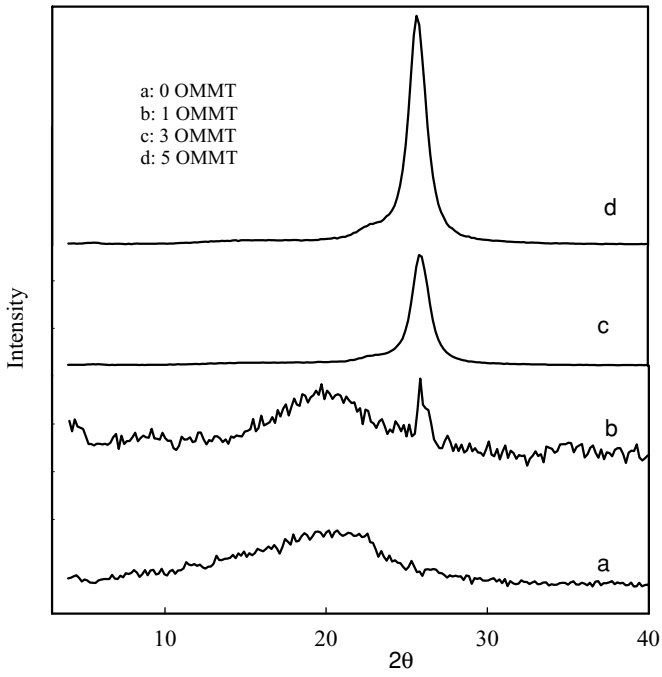

Fig. 4. XRD patterns of pure CS/ACMO and nanocomposites with different OMMT contents.

at (2 θ) 20° were observed and has abroad peak at $2\theta = 14.79$ with some amorphous characterization and reduction of crystalline of CS/ACMO compared to CS. Figure 4 is the XRD patterns of the pure CS/ACMO and the CS/ACMO/OMMT nanocomposites with different OMMT contents: (a) 0 wt% (PURE); (b) 1 wt% (1 OMMT); (c) 3 wt% (3 OMMT) and, (d) 5 wt% (5 OMMT). when the amount of the OMMT dispersed in CS/ACMO is only 1 wt%, peak at $2\theta = 14.79°$ still exist, but the intensity was reduced, in addition to the appearance of much more intense of new peak at $2\theta = 22.8°$ which means that the intercalation has occurred and the intercalated nanocomposites have been formed. With the amount of the OMMT increased to 5 wt%, there is no remarkable shift, indicating that the distance between the sheets of the CS/ACMO/OMMT is not affected by adding any amount of the OMMT.

3.4 SEM

Figure 5 shows the SEM image for the surface of CS/ACMO copolymer and its nancomposite containing 5% OMMT. The scanning showed that the particles of OMMT were agglutinated on the surface and intercalating with network structure of copolymer. Therefore, the nanocomposite appeared the surface as a rough surface which increases the activity of its surface by metal oxides exciting more than the surface of the copolymer CS/ACMO without OMMT which appeared as a smooth surface.

3.5 Thermal Analysis

Thermogravimetric analysis (TGA) of the prepared CS/ACMO and the polymeric phosphonium (CS/ACMO/OMMT) (5 wt%) nanocomposites were measured its thermal stability. TGA data in Figure 6 indicates that the (CS/ACMO/OMMT) decompose at a higher temperature in three stages with good thermal properties if compared with the CS/ACMO before it intercalate with OMMT which is undergo decomposition at relatively low temperature. Evidently, the onset temperature of that nanocomposite shift towards the higher temperature compared to the pure CS/ACMO, indicating the enhancement of thermal stability of the nanocomposites. This is a possible reason why MMT, with high thermal stability and great barrier properties of the nanolayers, is dispersed in the nanocomposites and prevents the heat to be transmitted quickly and limited any further continuous decomposition of the nanocomposites.

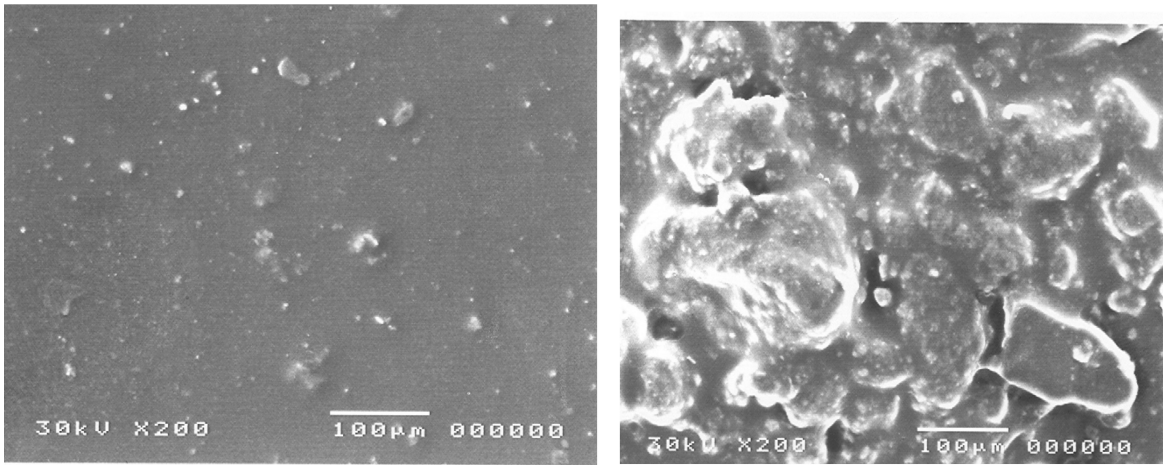

Fig. 5. Scanning electron micrography of (a) CS/ACMO and (b) CS/ACMO/OMMT (5% OMMT).

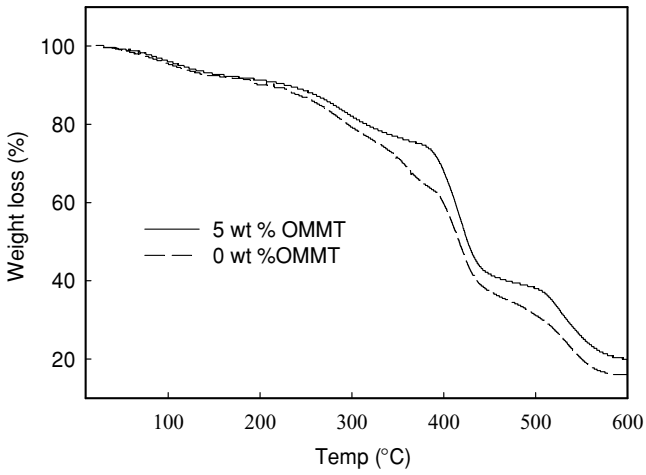

Fig. 6. Thermogravimetric analysis of CS/ACMO and CS/ACMO/OMMT (5 wt%) nanocomposites.

3.6 Water Uptake Studies

Table 1 shows the percentage of water uptake for the CS/ACMO/OMMT nanocomposites. It shows the decreasing trend of water uptake percentage with the increase of OMMT concentration. This is probably because OMMT can reduce the inter volume space among the chains leading to reducing the water uptake. Also, OMMT can be form high density of crosslinking sites which results in a crosslinking network structure.

3.7 Adsorption of Dye Pollutants

To study the adsorption of the dyes, CS/ACMO/OMMT nanocomposites with a different content of OMMT were placed in aqueous solutions of anionic dyes such as acid green B and acid fast yellow G (characteristic by presence of sulphonic SO_3H and mono-azo groups) and allowed to equilibrate for 24 h. At the end of this time, CS/ACMO/OMMT nanocomposites immersed in aqueous solutions of two acid dyes with initial concentration 100 mg/l showed a remarkable adsorption. The amounts adsorbed per unit mass of the hydrogels were calculated by using the following equation:

$$q_e = \left(\frac{C_i - C}{m}\right) \times V_t$$

where q_e is in mg adsorbate per gram of dry adsorbent, C_i and C are the initial and equilibrium concentrations of adsorbate solution (mg/l), V_t is the volume of solution treated (ml), and m is the mass of dry adsorbent (g).

Table 1. Water absorption of CS/ACMO/OMMT nanocomposites

OMMT conc. (wt%)	0	1	3	5
Water uptake (%) 24 h.	2143	1568	1531	1519

Table 2. Some sorption properties of CS/ACMO/OMMT nanocomposites

	Acid green B			*Acid fast yellow G*		
OMMT conc. (wt%)	C_e *(mg/l)*	q_e *(mg/g)*	K_d	C_e *(mg/l)*	q_e *(mg/g)*	K_d
0	18.9	30.9	4.3	66.2	19.3	0.5
1	21.2	55.9	3.7	61.5	26.5	0.6
3	8.6	74.9	10.6	38.5	54.7	1.6
5	5.9	51.7	16.0	18.0	42.4	4.6

The partition coefficient of the solute in solution and on adsorbent, K_d was calculated as;

$$K_d = C_m/C_s$$

Here C_m is the concentration of the salute in the hydrogel; C_s is the concentration in the solution after equilibrium has been reached. The equilibrium concentration in the solution (C) (mg ml^{-1}), the mass of adsorbed dyes in mg per mass of dry hydrogel in g resulting in (q_e) and the partition coefficient of the dyes (K_d) between solution and hydrogels were calculated and tabulated in Table 2.

In Table 2, it is shown that the value of partition ratio of acid fast yellow G is smaller than that of acid green B. Acid green B is anionic in character and containing charged chlorine ions and more than one sulfonate group. These results in charged and polarity sites enhanced the interaction with polar and charged phosphonium nanocomposite CS/ACMO/OMMT which is cationic in its structure by containing quaternary phosphonium groups. According to these results, it assumed that in the adsorption mechanism, hydrogen bonding, hydrophobic interactions (pollutant–polymer and pollutant–pollutant interactions), complexation and acid–base interactions between the sorbent and the pollutant, physical adsorption due to the polymer network and chemical interactions of solute dyes via ion exchange are all involved (29).

Table 2 shows the effect of OMMT wt% on adsorption capacity of CS/ACMO/OMMT nanocomposites for two acid dyes for C_i 100 mg/l, T: 30°C, t: 24 h. It is clear that wt% of OMMT including in nanocomposite is an important factor affecting adsorption capacity of the nanocomposite. As can be seen from Table 2, the adsorption capacity of the nanocomposite increased from 30.86 mg/g to 74.89 mg/g in acid green B and 19.34 mg/g to 54.70 mg/g in acid fast yellow G, with increasing OMMT from 0 wt% to 3 wt%. Phosphonium groups of OMMT participated in the polymerization and the formation of the intercalation nanostructure in CS/ACMO/OMMT, which may improve the polymeric network, and then enhance the adsorption capacity. However, the adsorption capacities of the nanocomposites decrease with further increasing wt% of OMMT when it exceeds 3 wt%. The lower tendency of

the adsorption capacity with increasing wt% may be attributed to the facts that the interaction among OMMT, CS and ACMO became intensive gradually with increasing wt%. Consequently, more chemical and physical crosslinkages were formed in the polymeric network, and then elasticity of the polymer chains decreases, which decreased the adsorption capacity of the nanocomposite (30).

3.8 Antimicrobial Activity of Polymeric Nanocomposite

Polymeric quaternary phosphonium compounds exhibit higher bacterial activity (22, 31). It is quite remarkable that quaternary phosphonium compounds are more effective against Staph. aureus and E. collie. Staph. aureus is normally more resistant to antimicrobials than E. coli. As can be seen from Table 3, the E. coli strain shows a higher killed as a higher inhibition in a clear circular zone than Staphylococcal colonies, while the Aspergillus fungus showed the most resistance by the copolymer and nanocomposits disks.

This result can be attributed to the chemical structures effects of copolymer and its nanocomposit on the cell wall composition of each microorganism. The electrostatic interactions between the positive charge of the polymer-phosphonium groups and the species negatively charged from the cellular membrane (32) play an important role in the adsorption at the active centers and in stopping the growth of bacterial cells. In general it can be stated that gram-positive bacteria have a very thick cellular wall made of many layers of peptide glycan. Gram-negative bacteria on the other hand, have cellular walls consisting of only a few layers of peptide glycan surrounded by an outer membrane of lipo polysaccharide. On other side, Asperagellus flavaus fungus showed higher resistance for copolymer and its nanocomposits due to high rigidity in its multilayer of cellular wall structure. The weak clear zone near the disk was attributed to only the hydrophilic copolymer effect to absorb water surrounded fungi molds therefore; it cannot grow in moisture depression conditions (33).

A more recent approach was realized by copolymer modifications that kill microbes on contact without releasing an exhaustible antimicrobial compound. Such systems are based on quaternary phosphonium copolymer, in which the antimicrobial activity group is a part of the copolymer backbone. The mechanism of QPCs action on the microorganism represented that polymeric QPCs cannot be absorbed, since the molecules are too large for this, therefore; they can immobilized and disrupt the cell membrane from the outside and on other side the microbial resistance does not occur in immobilized state (34).

Table 3. Antimicrobial activity of CS/ACMO/OMMT nanocomposites against different organisms

Tested microorganisms	*Diameter of inhibition zone (cm) produced by the copolymer (CS/ACMO/OMMT)*			
	0 OMMT	*1 OMMT*	*3 OMMT*	*5 OMMT*
Escherichia coli (−ve)	1.9	2.4	2.8	3.76
Staphylococcus aurius (+ve)	0.2	2.4	3.2	3.8
Aspergillus flavaus fungus	0.1	0.2	0.4	0.6

4 Conclusions

It can be concluded that the CS/ACMO/OMMT nanocomposites can be successfully prepared by γ-ray irradiation polymerization. XRD shows that the layers of MMT are intercalated and orderly dispersed in this nanocomposite. The nanocomposites exhibit an improvement of the thermal properties, and resistance to water uptake. Results of sorption experiments showed that CS/ACMO/OMMT nanocomposites exhibited high sorption capacities toward acid green B which contains more than one sulfonate group. According to these results, it assumed that in the adsorption mechanism, hydrogen bonding, hydrophobic interactions (pollutant–polymer and pollutant–pollutant interactions), complexation and acid–base interactions between the sorbent and the pollutant, physical adsorption due to the polymer network and chemical interactions of solute dyes via ion exchange are all involved. The polymer-bound phosphonium salts were proved to have antibacterial activity against *S. aureus*, *E. coli* and Aspergillus flavaus fungus.

References

1. Yao, K.J., Song, M., Hourston, D.J. and Luo, D.Z. (2002) *Polymer*, 43, 1017–1020.
2. Sun, T. and Garces, J.M. (2002) *Adv. Mater,* 14, 128–130.
3. Usuki, A., Tukigase, A. and Kato, M. (2002) *Polymer*, 43, 2185–2189.
4. Wu, J.H. and Lerner, M.M. (1993) *Chem. Mater.,* 5, 835–838.
5. Yano, S., Kurita, K., Iwata, K., Furukawa, T. and Kodomari, M. (2003) *Polymer*, 44, 3515–3522.
6. Kickelbick, G. (2003) *Prog Polym Sci.*, 28, 83–114.
7. Matejka, L., Dukh, O., Meissner, B., Hlavata, D., Brus, J. and Strachota, A. (2003) *Macromolecules*, 36, 7977–7785.
8. Mansur, H.S., Vasconcelos, W.L., Lenza, R.S., Oréfice, R.L., Reis, E.F. and Lobato, Z.P. (2000) *J. Non-Cryst Solids*, 273, 109–115.
9. Sarmento, V.H.V., Dahmouche, K., Santilli, C.V., Pulcinelli, S.H. and Craievich, A.F. (2003) *J. Appl. Cryst.*, 36, 473–477.
10. Ricciaedi, R., Auriemma, F., De Rosa, C. and Laupretre, F. (2004) *Macromolecules*, 37(5), 1921–1927.
11. Shahidi, F., Arachchi, J.K.V. and Jeon, Y.J. (1999) *Trends in Food Science & Technology*, 10, 37–51.
12. Vilivalam, V.D. and Dodane, V. (1998) *Pharmaceutical Science & Technology Today*, 6, 246–253.
13. Ravi, K. and Majeti, N.V. (2000) *Reactive and Functional Polymers*, 1, 1–27.
14. Lopez, C. R. and Bodmeier, R. (1997) *Journal of Controlled Release*, 44, 215–225.

15. Perugini, P., Genta, I., Conti, B., Modena, T. and Pavanetto, F. (2003) *International Journal of Pharmaceutics*, 252, 1–9.
16. Rujiravanit, R., Kruaykitanon, S., Jamieson, A.M. and Tokura, S. (2003) *Macromolecule Bioscience*, 3, 604–611.
17. Wang, J.W. and Hon, M.H. (2005) *Journal of Applied Polymer Science*, 96, 1083–1094.
18. Li, Z., Du, Y.M., Zhang, L.N. and Pang, D.W. (2003) *Reactive and Functional Polymers*, 55, 35–43.
19. Kojima, Y., Usuki, A., Kawasumi, M., Okada, A., Fukushima, Y., Kurauchi, T. and Kamigaito, O. (1993) *J. Mater. Res*., 8(5), 1185–1189.
20. Wang, M.S. and Pinnavaia, J. (1994) *J. Chem. Mater*., 6(4), 468–474.
21. Salahuddin, N. and Akelah, A. (2002) *Polym. Adv. Technol*., 13, 339–345.
22. Kanazawa, A., Ikeda, T. and Endo, T. (1993) *J. Polymer Sci, Part A, Polymer Chem*., 31(2), 335–343.
23. Kanazawa, A., Ikeda, T. and Endo, T. (1993) *J. Polymer Sci, Part A: Polymer Chem*., 31(11), 2873–2876.
24. Akelah, A. and Moet, A. (1996) *Journal of Materials Science*, 31(13), 3589–3596.
25. Adriana, Pop, Davidescu, C.M., Trif, R., Ilia, Gh., Smaranda, Iliescu, and Dehelean, Gh. (2003) *Reactive & Functional Polymers*, 55, 151–158.
26. Madejova, J. (2003) *Vibrational Spectroscopy*, 31, 1–10.
27. Tyagi, B., Chudasama, C.D. and Jasra, R.V. (2006) *Spectrochimica Acta Part A, Molecular and Biomolecular Spectroscopy*, 64(2), 273–278.
28. Devika, R.B. and Varsha, B.P. (2006) *Pharm. Sci.Tech.*, 7(2), Article 50 (http://www.aapspharmscitech.org).
29. Abdel-Aal, S.E., Hegazy, E.A., Abou Taleb, M.F. and Dessouki, A.M. (2008) *Journal of Applied Polymer Science*, 107(3), 1759–1776.
30. Wang, L., Zhang, J. and Wang, A. (2008) *Colloids and Surfaces A: Physicochem. Eng. Aspects*, article in press.
31. Tashiro, T. (2001) *Macromolecules Macromol. Mater. Eng.,* 286(2), 63–87.
32. Daniels, S.L., in: Gitton, G., Marshall, K.C. (Eds.), Adsorption of Microorganism to Surfaces, Wiley, New York, p. 7, 1980.
33. Andreas, D.F. and Joerg, C.T. (2006) *Angew. Chem. Int. Ed.,* 45, 6759–6762.
34. Miloviǵ, N.M., Wang, J., Lewis, K. and Klibanov, A.M. (2005) *Biotechnol. Bioeng*., 90(6), 715–722.